Journal of Software Engineering

ISSN 1819-4311

Academic Journals Inc.

www.academicjournals.com

Journal of Software Engineering 9 (4): 735-748, 2015
ISSN 1819-4311 / DOI: 10.3923/jse.2015.735.748

Heat Flux Equation and Characteristics of Heat and Mass Transfer of Evaporating Meniscus

[1]Guochang Zhao, [1]Lei Cao, [2]Liping Song and [1]Tiandong Lu
[1]Faculty of Aerospace Engineering, Shenyang Aerospace University, Shenyang, 110136, China
[2]Institute of Higher Education, Shenyang Aerospace University, Shenyang, 110136, China

Corresponding Author: Guochang Zhao, Faculty of Aerospace Engineering, Shenyang Aerospace University, Shenyang, 110136, China

ABSTRACT

The governing equations for heat and mass transfer of evaporating meniscus are derived and solved by fourth-order Runge-Kutta method. The equation for evaporating heat flux is originally derived in thermal resistance form and it is found that the key factors that affect the heat transfer of intrinsic meniscus are surface tension and conduction thermal resistance of the liquid film; the suppressing effects of disjoining pressure and surface tension are very strong. The disjoining pressure predominates in extremely thin films while the evaporation driving effect of temperature difference between the wall and vapor is dominant in relatively thicker films. Other factors such as groove width, superheat, surface tension coefficient, latent heat of evaporation, kinetic viscosity and acceleration are analyzed as well. For acceleration, Bond number is introduced to evaluate its influence on the heat transfer of evaporating meniscus.

Key words: Evaporation, film, interfacial tension, thermal resistance, disjoining pressure

INTRODUCTION

Heat and mass transfer characteristics of the evaporating meniscus is of key importance to heat pipes utilizing micro grooves and other heat exchangers based on interfacial phenomena. In evaporating thin film, the heat flux peak can reach an order of magnitude of 10^6-10^7 $W \cdot m^{-2}$, the contribution of evaporating thin film to the overall heat transfer is more than 20% and can increase when the groove size is bigger or superheat is smaller (Wang *et al*., 2007). Such high heat flux is extremely desirable for heat dissipation of microelectronic chips and other compact heat exchanger. Consequently, the flow and heat transfer in the vicinity of the meniscus has been widely studied. The film thickness of evaporating meniscus can range from nanometers in the case of equilibrium thin film to half of the microgroove width in the case of intrinsic meniscus and the film shape is closely associated with groove width, properties of substrate and working fluid, boundary conditions, etc. Accordingly, to measure the thickness and shapes of the meniscus requires that the experimental setup has the ability to measure the film thickness varies across several orders of magnitude. Furthermore, to obtain a fairly steady state evaporating liquid film is even more difficult than to measure the thickness and shapes of the meniscus. Due to above experimental research difficulty, the theoretical research can be an important complement. Wayner and co-workers (Wayner and Coccio, 1971; Potash and Wayner Jr., 1972; Wayner *et al*., 1976; Preiss and Wayner Jr., 1976; Wayner, 1979; Wayner *et al*., 1985; Truong and Wayner Jr., 1987;

Sujanani and Wayner Jr., 1991; Wayner, 1991; Schonberg and Ayner, 992; Sujanani and Wayner Jr., 1992; Wayner, 1994) carried out extensive theoretical and experimental studies. They used Kelvin equation (Dasgupta *et al.*, 1994) and Clausius-Clapeyron Equation (Wayner, 1991) to simplify the equation established by Schrage (1953) and combined the extended Young-Laplace equation (Dasgupta *et al.*, 1993) to derive a new concise equation, which is widely used in the theoretical study of evaporating meniscus. Wang *et al.* (2008) used Runge-Kutta method to solve the fourth-order Ordinary Differential Equation (ODE) of liquid film thickness. Du and Zhao (2011) proposed a more reasonable second-order initial condition and analyzed the influence of several factors on heat transfer of thin liquid film.

In this study, an evaporating meniscus in a rectangular microgroove is investigated. Based on previous studies, the governing equations are derived and solved with Runge-Kutta method. The equation of evaporation heat flux is rewritten into the thermal resistance form, in order to reasonably clarify the driving and suppressing mechanisms of evaporative heat transfer and to examine the effects of evaporative thermal resistance and conduction thermal resistance of the liquid film on the heat transfer of the evaporating meniscus. Finally, referring to the above results, several factors influencing the evaporation heat transfer are analyzed.

THEORETICAL MODEL

Since the film shape and controlling force varies along the evaporating meniscus, it is typically divided into three regions as illustrated in Fig. 1 (Potash and Wayner Jr., 1972). An intrinsic meniscus, with the thickest film, where the surface curvature radius is deemed as constant and surface tension plays a dominant role; an evaporating thin film, as liquid flowing from intrinsic meniscus across this region, where the thickness of liquid film rapidly decreases and the disjoining pressure which defined by Derjaguin and Churaev (1978) will increase sharply to replace the surface tension as the leading role; an equilibrium thin film or adsorbed layer located at the leading edge of evaporating meniscus with film thickness equals to several diameters of molecule, where no evaporation occurs as liquid molecules can seldom escape from the vapor-liquid interface.

Assumptions: In order to simplify the analyses, it is necessary to make the following assumptions: (1) Constant thermal properties of liquid and vapor, (2) Steady incompressible laminar flow in evaporating meniscus, (3) One-dimensional heat conduction and evaporation is considered and the

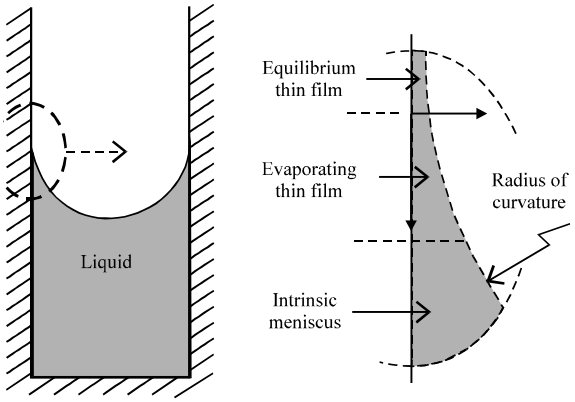

Fig. 1: Schematic diagram of evaporating meniscus in micro groove

convection is ignored, (4) The vapor is saturated and its pressure and temperature is uniform everywhere, (5) Uniform wall temperature, (6) Nonpolar working fluid, (7) Ignore the Marangoni effect, (8) Liquid wets the wall completely.

Governing equations

Momentum conservation equation: The two-dimensional momentum conservation equation in x direction is:

$$\rho_l\left(\frac{\partial u}{\partial t}+u\frac{\partial u}{\partial x}+v\frac{\partial u}{\partial y}\right)=\rho_l g_x-\frac{\partial P_l}{\partial x}+\mu_l\left(\frac{\partial^2 u}{\partial y^2}+\frac{\partial^2 u}{\partial x^2}\right) \quad (1)$$

Since the process is considered to be a steady process, so $\partial u/\partial\tau = 0$. The flow is laminar and velocity and film thickness is small, thus the inertial term can be ignored, namely, $u(\partial u/\partial x)+v(\partial v/\partial y)\approx 0$. Based on Prandtl's boundary layer theory, magnitude analysis can be completed on the momentum equation (Moosman and Homsy, 1980) to get: $\partial^2 u/\partial x^2\approx 0$, $\partial P_l/\partial y\approx 0$, which means P_l is only related to x. The equation simplifies to:

$$\frac{dP_l}{dx}=\rho_l g_x+\mu_l\frac{\partial^2 u}{\partial y^2} \quad (2)$$

The flow boundary conditions are as follows:

$$u|_{y=0}=0 \ \text{(no slip)} \ \square\frac{\partial u}{\partial y}|_{x=\delta}=0 \quad (3)$$

No vapor-liquid interfacial shear stress.

From the momentum Eq. 1, the following equations (Eq. 4-16) can be derived according to their relationship.

Mass balance equation: According to Eq. 3, two integrals will be carried out for Eq. 2 (limit of integration from 0 to y) to obtain the velocity along the x direction:

$$u=\frac{1}{u_l}\left(\frac{dP_l}{dx}-\rho_l g_x\right)\left(\frac{1}{2}y^2-\delta y\right) \quad (4)$$

The mass flow rate must satisfy the following equation:

$$m_x=-\rho_l\int_0^\delta u\,dy=\frac{\delta^3}{3v_l}\left(\frac{dP_l}{dx}-\rho_l g_x\right) \quad (5)$$

To ensure the mass flow rate is positive, a minus sign is added on the right side of the equal sign in Eq. 5, it is a consequence of the fact that the fluid velocity is in the opposite x direction. The dp_l/dx is determined by the following force balance equation.

Force-balance equation: An augmented Young-Laplace equation can be obtained for force balance in the thin film by introducing disjoining pressure, which is:

$$P_v - P_l = P_c + P_d = \frac{\sigma}{r} + P_d \tag{6}$$

where pressure difference between liquid and vapor is resulted from the combined effect of surface tension P_c and disjoining pressure P_d. The σ and r denote surface tension coefficient and curvature radius, respectively.

The relationship between curvature and curvature radius is:

$$K = \frac{1}{r} = \frac{d^2\delta}{dx^2}\left[1+\left(\frac{d\delta}{dx}\right)^2\right]^{-3/2} \tag{7}$$

For nonpolar liquid, the disjoining pressure is expressed as:

$$P_d = \frac{A}{\delta^3} \tag{8}$$

where, A is dispersion constant. According to assumption Eq. 4, vapor pressure P_v is constant, then, the derivative of Eq. 6 can be written as:

$$\frac{dP_l}{dx} = -\left[\frac{d}{dx}\left[\frac{\sigma}{r}\right] + \frac{dP_d}{dx}\right] \tag{9}$$

Combining Eq. 7 and 8 with Eq. 9, a third-order differential equation is expressed as:

$$\delta''' - \frac{3\delta'(\delta'')^2}{1+(\delta')^2} + \frac{1}{\sigma}\left(\frac{dP_l}{dx} - \frac{3A}{\delta^4}\delta'\right)(1+(\delta')^2)^{1.5} = 0 \tag{10}$$

where, the liquid pressure gradient P_l is a function of liquid film thickness.

Evaporation rate equation: Due to evaporation, the mass flow rate which supported by the pressure gradient decreases during the flow process and the expression can be written as:

$$\frac{d\dot{m}_x}{dx} = \dot{m}_e \tag{11}$$

where, m_e is the evaporating mass flux. Now, the relationship between the flow and evaporation is established. By simplifying Schrage (1953) original equation (Wayner *et al*., 1976). Proposed the following equation:

$$\dot{m}_e = a(T_{lv} - T_v) - b\,(P_d + P_c) \tag{12}$$

Where:

$$a = C\left[\frac{M}{2\pi R T_{lv}}\right]^{\frac{1}{2}} \frac{P_v h_{fg}}{R_g T_{lv} T_v}$$

$$b = C\left[\frac{M}{2\pi R T_{lv}}\right]^{\frac{1}{2}} \frac{P_v}{R_g T_{lv} \rho_l}$$

are coefficients, which depend on the properties and state of the fluid.

Energy-balance equation: Evaporative heat flux and evaporative mass flux have the following relation:

$$\ddot{q} = \ddot{m}_e h_{fg} \tag{13}$$

Under steady state conditions, the evaporative heat flux equals to the heat conducted through the liquid film:

$$\ddot{q} = \frac{T_w - T_{lv}}{\delta / \lambda_l} \tag{14}$$

Combining Eq. 12, 14 and 15 can be obtained:

$$\ddot{m}_e = \frac{1}{1 + a h_{fg} \delta / \lambda_l}\left[a(T_w - T_v) - b(P_d - P_c)\right] \tag{15}$$

Fourth-order ordinary differential equation: Based on the above equations, the flow and heat transfer parameters are functions of the thickness of liquid film. Thus, the first step to solve above equations is to obtain the thickness profile of liquid film. Combining Eq. 5, 9, 11 and 15, The fourth-order ordinary differential equation is expressed as:

$$d\left[\delta^3\left(\rho_l g_x + \frac{d}{dx}\left(\frac{\sigma}{r}\right) + \frac{dP_d}{dx}\right)\right] / dx = \frac{-3\nu_l}{1 + a h_{fg} \delta / \lambda_l}\left[a(T_w - T_v) - b(P_d - P_c)\right] \tag{16}$$

SOLUTION METHOD AND ANALYSES

The evaporating meniscus to be studied is the evaporation of Octane wetting the silicon substrate with groove width of 2.5 μm. Detailed parameters are shown in Table 1.

Boundary conditions: The Runge-Kutta method is employed to solve Eq. 16, a fourth-order non-linear ODE, which can be treated as an initial-value problem. To solve Eq. 16, four initial values are specified as follows:

Table 1: Properties and parameters of octane

Properties	Values	Properties	Values
A/J	3.18×10^{-21}	T_w/K	344
P_v/Pa	1.528×10^{4}	T_v/K	343
ρ_l/kg·m^{-3}	661.2	ν_l/m^2·s^{-1}	4.916×10^{-7}
λ_l/W·m^{-1}·K^{-1}	0.11	σ/N·m^{-1}	0.0216
h_{fg}/J·kg^{-1}	3.398×10^{5}	R_g/J·kg^{-1}·K^{-1}	72.79

- **Zero-order initial value:** The origin point (x = 0) is set at the conjunction of equilibrium thin film and evaporating thin film, where the evaporative rate is zero, $T_{lv}\tilde{}T_w$, $P_c<<P_d$. Substituting those into Eq. 12, the following is obtained:

$$\delta(0) = \sqrt[3]{\frac{AT_v}{h_{fg}\rho_l\,(T_w - T_v)}} \tag{17}$$

It should be noted that this $\delta(0)$ cannot be directly taken as the zero-order initial value and $1.1\delta(0)$ is used.

- **First-order initial value:** Since disjoining pressure is dominant in the region of equilibrium thin film, evaporation is almost completely suppressed causing the film thickness to be nearly constant and d'(0) is close to 0. The calculation indicates that the film shape is not sensitive to $\delta'(0)$, here the value is set as:

$$\delta'(0) = 10^{-11} \tag{18}$$

- **Second-order initial value:** The second order initial value is calculated by carrying out iterative calculations until the $\delta''(0)$ reaches a desirable accuracy and the calculation should meet certain far-field boundary condition Eq. 18. Our value is:

$$\delta''(0) = 2.24845369\times10^{5} \tag{19}$$

- **Third-order initial value:** Substituting the above three initial values into Eq. 10 and $\delta'(0)$ is:

$$\delta''(0) = 3.6696\times10^{5} \tag{20}$$

With the four initial values, the definite solution of Eq. 16 can be obtained.

Validation: The Octane parameters and the test data of film thickness come from Kim's dissertation (Kim, 1994) is used to validate our present model. The calculated results and the experimental data are shown in Fig. 2 and 3. The maximum relative error between Kim's data and our present model under two different heating powers is less than 6%.

Discussion on the boundary of evaporating thin film: Due to the fact that the boundaries of the evaporating thin liquid film and the start of intrinsic meniscus have several different

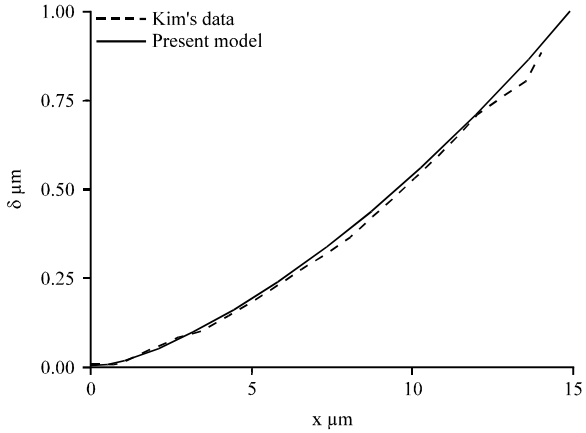

Fig. 2: Comparison between experimental and numerical results at Q = 14.28 W

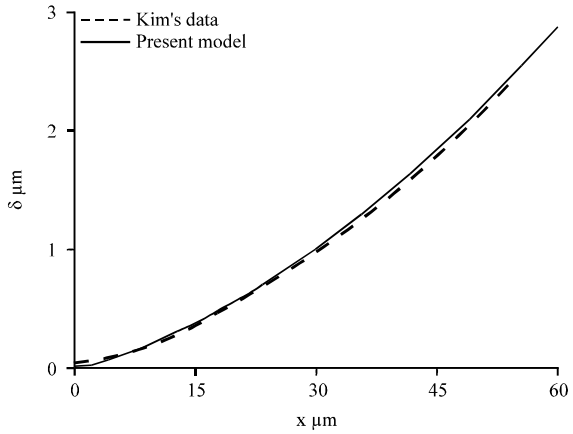

Fig. 3: Comparison between experimental and numerical results at Q = 5.65 W

definitions, it is necessary to make a clear explanation to avoid ambiguity. In this study, the boundary is defined as the location where the curvature radius approaches to a constant value. Here, the ratio P_d/P_c=1/1000 is set as the end of the evaporating thin film and compared with Wang's definition (1/2000 P_{do}) (Wang *et al.*, 2008), as shown in Fig. 4.

Heat transfer analyses: By introducing the thermal resistance, the evaporative heat flux equation can be rearranged as:

$$q = \left[\frac{1}{ah_{fg}} + \frac{\delta}{\lambda_l}\right]^{-1}\left[(T_w - T_v) - \frac{b}{a}(P_d + P_c)\right] \tag{21}$$

where, $1/(ah_{fg})$ is evaporative thermal resistance. T_w-T_v is the temperature difference which is the driving force behind the heat transfer and (P_d+P_c) b/a has a suppressing effect. From Eq. 21, it is easy to analyze the influence of various parameters on the evaporative heat transfer. The

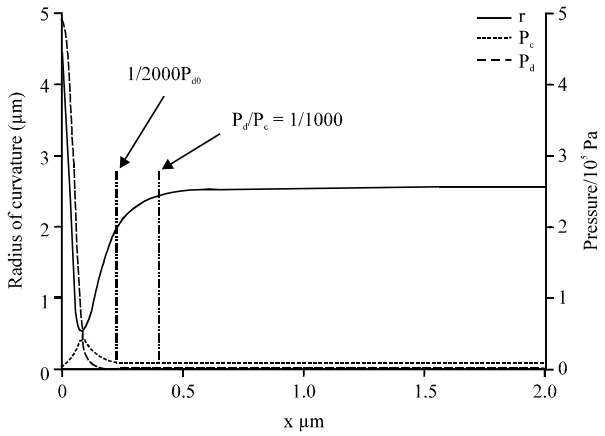

Fig. 4: Variation of pressure components and radius of curvature along the film

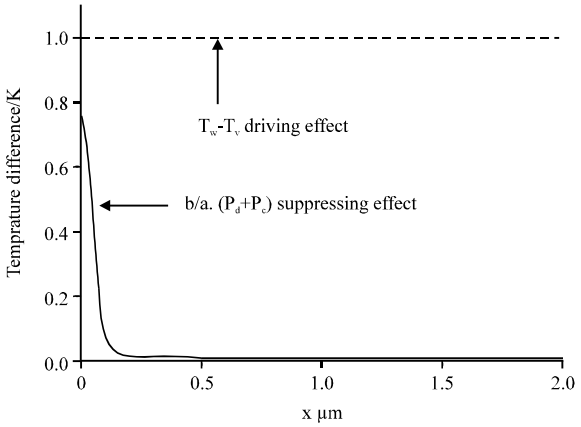

Fig. 5: Comparison of the driving and suppressing effect along the film

following is the detailed analyses which consist of evaporation with driving effect and suppressing effect, comparison of evaporative thermal resistance and conduction thermal resistance, relationship of evaporative heat flux, pressure and thermal resistances. In Fig. 5, the temperature difference between the wall and vapor is a constant 1K along the film based on the assumptions made. In the region with ultrathin liquid film, the drive effect and suppressing effect is of the same order of magnitude. As the film thickness increases, the disjoining pressure decreases sharply, thus, its suppressing effect weakens rapidly while the suppressing effect of surface tension fluctuate slightly. This transition occurs in the region of evaporating thin film. As for intrinsic meniscus region, the disjoining pressure has reduced greatly and the evaporation in this region is mainly related to temperature difference.

The evaporative heat resistance $1/(a \cdot h_{fg})$ can be regarded as constant since it is decided by the properties and under the unchanged the operating condition. The conduction thermal resistance is the ratio between film thickness and thermal conductivity coefficient of the liquid. As shown in Fig. 6, in the region of evaporating thin film, the evaporative thermal resistance is far bigger than the conduction thermal resistance and the latter increases as film thickens. At a certain location,

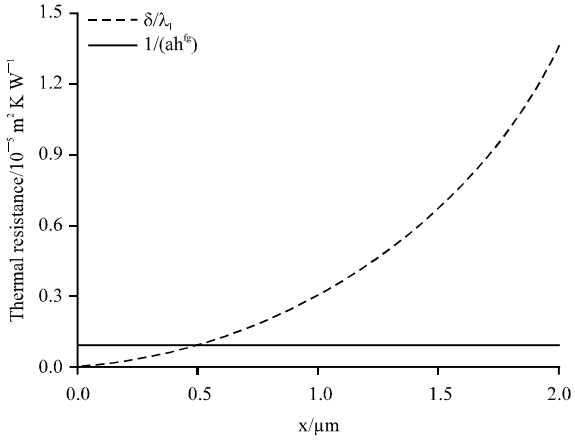

Fig. 6: Comparison of the two heat resistance along the film

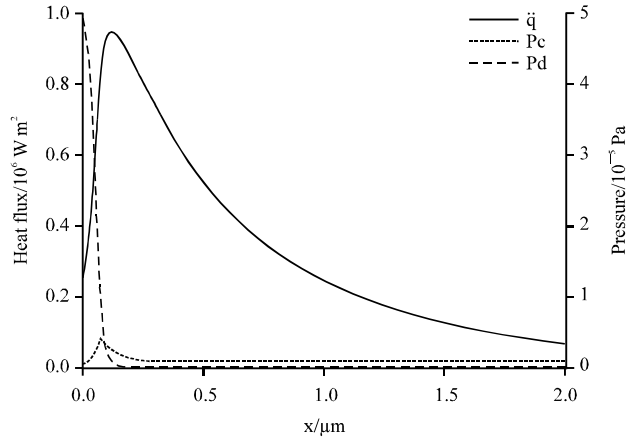

Fig. 7: Influence of pressure components on heat flux

the two thermal resistances equal each other. For present calculation, the location is at $x = 5\times10^{-7}$ m approximately and the film thickness δ is 1×10^{-7} m. As the film thickness continues to increase, the latter will replace the evaporative heat resistance as the main thermal resistance. This knowledge will provide a valuable reference for minimizing the thermal resistance. As shown in Fig. 7, the overall suppressing effect reduces sharply along the x direction whereas the total thermal resistance increase. The comprehensive effect is that a heat flux peak occurs in a local region. As the film thickness increases, the suppressing effect can be ignored and the heat flux equation becomes:

$$\ddot{q} = (1/ah_{fg} + \delta/\lambda_l)^{-1}(T_w - T_v) \tag{22}$$

If the conduction thermal resistance increases to the point that the evaporative thermal resistance become negligibly small, then Eq. 22 can be further simplified to:

$$\ddot{q} = (\delta/\lambda_l)\bullet(T_w - T_v) \tag{23}$$

ANALYSES OF FACTORS INFLUENCING HEAT TRANSFER

Groove width: The cumulative heat transfer rate is defined as:

$$\ddot{q} = \int_0^x \ddot{q}dx \tag{24}$$

In Fig. 8, for a single groove, it is seen that the heat transfer rate increases as the groove width increases but with a decreasing effect at greater groove widths. On the other hand, if the groove width is small, then the number of grooves increases. In general, the thinner the groove, the higher the heat transfer efficiency.

Superheat: Figure 9 shows that as superheat increases, the cumulative heat transfer rate increases with the same ratio. Here, superheat is defined as the temperature difference of solid wall and the vapor.

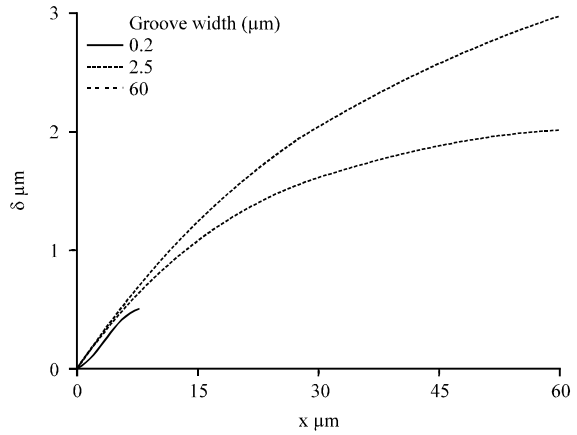

Fig. 8: Influence of groove width on cumulative heat transfer rate

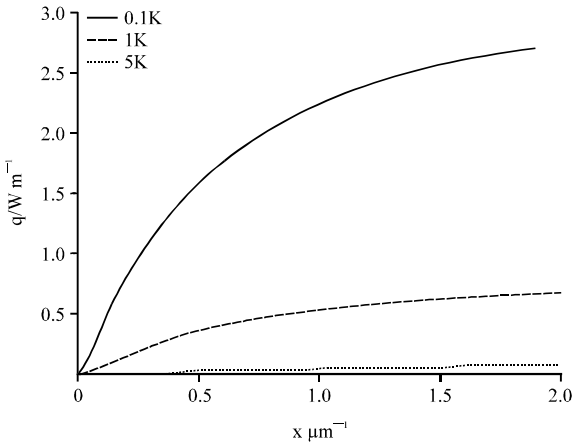

Fig. 9: Influence of super heat on cumulative heat transfer rate

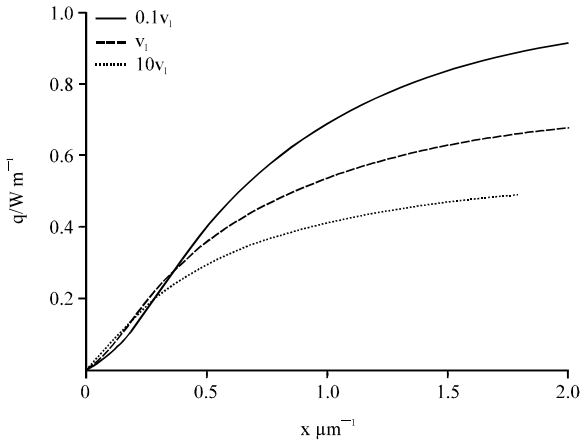

Fig. 10: Influence of surface tension on cumulative heat transfer rate

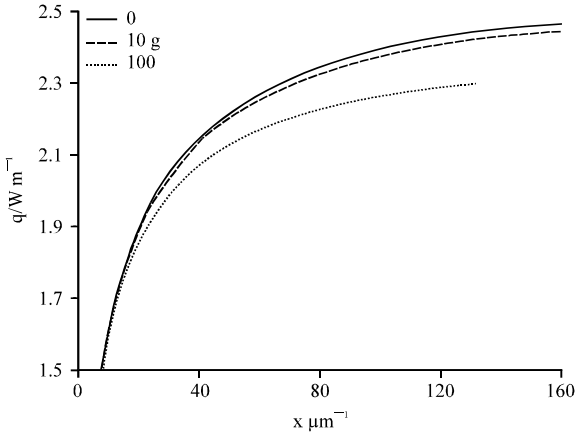

Fig. 11: Influence of latent heat of evaporation on cumulative heat transfer rate

Surface tension coefficient: It is found from the calculation that as the surface tension increase, the shape of liquid film tends to be flatter and evaporative heat flux peak drops slightly. This effect can be attributed to the increase of surface tension which strengthens the suppressing effect and the conduction thermal resistance decreases since the film shape becomes smoother, so the evaporative heat flux increases moderately in the thicker film region, which is shown in Fig. 10. The cumulative heat transfer rate increases and the influence of surface tension is mainly effective in the region with thicker liquid film.

Latent heat of evaporation: As shown in Fig. 11, along with the increase of the latent heat of evaporation, the evaporative heat transfer rate increases with a greater rate of increase in thinner film regions. This is consistent with the fact that the latent heat of evaporation is directly related to the evaporative thermal resistance and it mainly affects heat transfer in the evaporating thin film.

Kinetic viscosity: According to Eq. 5, it can be concluded that the flow resistance increases with increasing kinetic viscosity and this directly leads to the decrease of evaporation rate, This

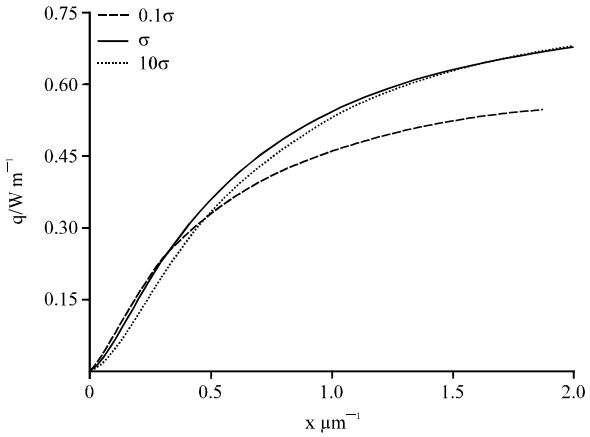

Fig. 12: Influence of kinetic viscosity on cumulative heat transfer rate

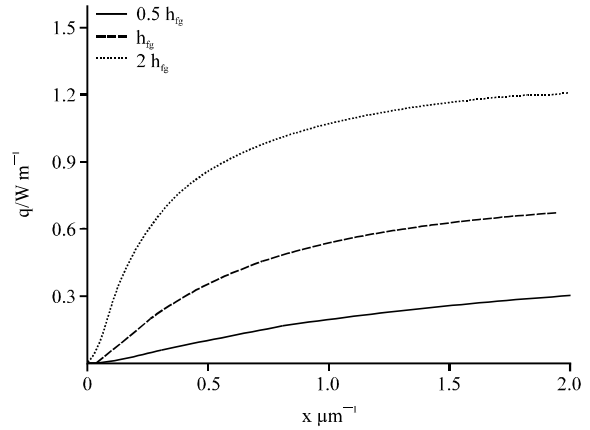

Fig. 13: Influence of acceleration on cumulative heat transfer rate

conclusion means that a larger pressure gradient is required to maintain the same evaporation rate. In addition, from Eq. 9, pressure gradient is the sum of surface tension gradient and disjoining pressure gradient, which means that the liquid film shape is steeper and thus the conduction thermal resistance is bigger. The comprehensive effect is that the bigger the viscosity, the smaller the heat transfer rate, which is shown in Fig. 12.

Acceleration: The groove width considered here is 0.4 mm. It is found that the heat transfer rate is almost the same under gravity and weightlessness condition. As shown in Fig. 13, when acceleration increases to 10 g, its influence is extremely weak and up to 100 g, is noticeable in the intrinsic meniscus region.

The Bond Hager (2012) number (abbreviated as Bo) is introduced to evaluate the influence of acceleration. Bo is define as $Bo = gL^2 \cdot (\tilde{n}_l - \tilde{n}_v)/\sigma$, where g is acceleration of gravity and L is the characteristic length which in this case is the groove length. Bo indicates the ratio of gravity and surface tension. In this study, the gravity is extended to arbitrary acceleration and accelerations

of 0, 10, 100 g are considered. For 10 and 100 g, Bo is 0.5 and 5, respectively. It can be concluded that when Bo approaches about 1, the influence of acceleration appears and the bigger the Bo, the more obvious the influence.

CONCLUSION

(1) A model of an evaporating meniscus is validated by comparing with the experimental data in existing literature and numerically solved. (2) The evaporative heat flux equation is rearranged into thermal resistance form. It is found that the evaporation process is driven by the temperature difference between solid wall and vapor and suppressed by disjoining pressure and surface tension. Evaporative thermal resistance and conduction thermal resistance of liquid film are the main thermal resistances. The disjoining pressure and evaporative thermal resistance dominant the heat transfer in evaporating thin film and the surface tension and the conduction thermal resistance of liquid film govern the heat transfer in intrinsic meniscus region. (3) On the basis of the above conclusions, several factors affecting the heat transfer are briefly analyzed.

ACKNOWLEDGMENT

This study is supported by Scientific Research Foundation for Liaoning Province Pandeng Scholars (2013, 2015) and the Aviation Science Foundation of China (20131954004).

REFERENCES

DasGupta, S., J.A. Schonberg, I.Y. Kim and P.C. Wayner Jr., 1993. Use of the augmented Young-Laplace equation to model equilibrium and evaporating extended menisci. J. Colloid Interface Sci., 157: 332-342.

DasGupta, S., I.Y. Kim and P.C. Wayner Jr., 1994. Use of the Kelvin-Clapeyron equation to model an evaporating curved microfilm. J. Heat Transfer, 116: 1007-1015.

Derjaguin, B.V. and N.V. Churaev, 1978. On the question of determining the concept of disjoining pressure and its role in the equilibrium and flow of thin films. J. Colloid Interface Sci., 66: 389-398.

Du, S.Y. and Y.H. Zhao, 2011. New boundary conditions for the evaporating thin-film model in a rectangular micro channel. Int. J. Heat Mass Transfer, 54: 3694-3701.

Hager, W.H., 2012. Wilfrid noel bond and the bond number. J. Hydraulic Res., 50: 3-9.

Kim, I.Y., 1994. An Optical Study of the Heat Transfer Characteristics of an Evaporating Thin Liquid Film. Rensselaer Polytechnic Institute, New York, Pages: 422.

Moosman, S. and G.M. Homsy, 1980. Evaporating menisci of wetting fluids. J. Colloid Interface Sci., 73: 212-223.

Potash, Jr. M. and P.C. Wayner Jr., 1972. Evaporation from a two-dimensional extended meniscus. Int. J. Heat Mass Transfer, 15: 1851-1863.

Preiss, G. and P.C. Wayner Jr., 1976. Evaporation from a capillary tube. J. Heat Transfer, 98: 178-181.

Schonberg, J.A. and P.C. Ayner, 1992. Analytical solution for the integral contact line evaporative heat sink. J. Thermophys. Heat Transfer, 6: 128-134.

Schrage, R.W., 1953. A Theoretical Study of Interphase Mass Transfer. Columbia University Press, New York, Pages: 103.

Sujanani, M. and P.C. Wayner Jr., 1991. Microcomputer-enhanced optical investigation of transport processes with phase change in near-equilibrium thin liquid films. J. Colloid Interface Sci., 143: 472-488.

Sujanani, M. and P.C. Wayner Jr., 1992. Transport processes and interfacial phenomena in an evaporating meniscus. Chem. Eng. Commun., 118: 89-110.

Truong, J.G. and P.C. Wayner Jr., 1987. Effects of capillary and van der Waals dispersion forces on the equilibrium profile of a wetting liquid: Theory and experiment. J. Chem. Phys., 87: 4180-4188.

Wang, H., S.V. Garimella and J.Y. Murthy, 2007. Characteristics of an evaporating thin film in a microchannel. Int. J. Heat Mass Transfer, 50: 3933-3942.

Wang, H., S.V. Garimella and J.Y. Murthy, 2008. An analytical solution for the total heat transfer in the thin-film region of an evaporating meniscus. Int. J. Heat Mass Transfer, 51: 6317-6322.

Wayner, Jr. P.C. and C.L. Coccio, 1971. Heat and mass transfer in the vicinity of the triple interline of a meniscus. AIChE J., 17: 569-574.

Wayner, Jr. P.C., 1979. Effect of thin film heat transfer on meniscus profile and capillary pressure. AIAA J., 17: 772-776.

Wayner, Jr. P.C., 1991. The effect of interfacial mass transport on flow in thin liquid films. Colloids Surfaces, 52: 71-84.

Wayner, Jr. P.C., 1994. Thermal and mechanical effects in the spreading of a liquid film due to a change in the apparent finite contact angle. J. Heat Transfer, 116: 938-945.

Wayner, Jr. P.C., C.Y. Tung, M. Tirumala and J.H. Yang, 1985. Experimental study of evaporation in the contact line region of a thin film of hexane. J. Heat Transfer, 107: 182-189.

Wayner, Jr. P.C., Y.K. Kao and L.V. LaCroix, 1976. The interline heat-transfer coefficient of an evaporating wetting film. Int. J. Heat Mass Transfer, 19: 487-492.